

# Identification of Waves by RF Magnetic Probes during Lower Hybrid Wave Injection Experiments on the TST-2 Spherical Tokamak<sup>\*)</sup>

Takahiro SHINYA, Akira EJIRI, Yuichi TAKASE, Takuma WAKATSUKI, Takuya OOSAKO, Naoto TSUJII, Hidetoshi KAKUDA, Hirokazu FURUI, Junichi HIRATSUKA, Takuma INADA, Kazuhiro IMAMURA, Keishun NAKAMURA, Ayaka NAKANISHI, Masateru SONEHARA, Hiro TOGASHI, Shintaro TSUDA, Takashi YAMAGUCHI, Hiroshi KASAHARA<sup>1)</sup>, Kenji SAITO<sup>1)</sup>, Tetsuo SEKI<sup>1)</sup>, Fujio SHIMPO<sup>1)</sup>, Yoshihiko NAGASHIMA<sup>2)</sup>, Osamu WATANABE<sup>2)</sup> and Takuma YAMADA<sup>2)</sup>

*The University of Tokyo, Kashiwa 277-8561, Japan*

<sup>1)</sup>*National Institute for Fusion Science, Toki 509-5292, Japan*

<sup>2)</sup>*Kyushu University, 6-1 Kasuga-koen, Kasuga, Fukuoka 816-8580, Japan*

(Received 16 December 2013 / Accepted 3 March 2014)

RF magnetic probes can be used to measure not only the wavevector, but also the polarization of waves in plasmas. A 5-channel RF magnetic probe (5ch-RFMP) was installed in the TST-2 spherical tokamak and the waves were studied in detail during lower hybrid wave injection experiments. From the polarization measurements, the poloidal RF magnetic field is found to be dominant. In addition to polarization, components of  $k$  perpendicular to the major radial direction were obtained from phase differences among the five channels. The radial wavenumber was obtained by scanning the radial position of the 5ch-RFMP on a shot by shot basis. The measured wavevector and polarization in the plasma edge region were consistent with those calculated from the wave equation for the slow wave branch. While the waves with small and large  $k_{\parallel}$  were excited by the antenna, only the small  $k_{\parallel}$  component was measured by the 5ch-RFMP; this suggests that the waves with larger  $k_{\parallel}$  were absorbed by the plasma.

© 2014 The Japan Society of Plasma Science and Nuclear Fusion Research

Keywords: RF magnetic probe, lower hybrid wave, spherical tokamak, wavevector, polarization

DOI: 10.1585/pfr.9.3402040

## 1. Introduction

Lower hybrid wave (LHW) is used to drive the plasma current in tokamaks. In the TST-2 spherical tokamak, the LHW is used to ramp up the plasma current non-inductively [1]. The LHW is often measured by electrostatic probes to confirm the electrostatic dispersion relation [2, 3]. In this study, we report the possibility of direct wavevector and polarization measurements of the LHW using a 5-channel RF magnetic probe (5ch-RFMP).

RFMPs have two advantages over electrostatic probes. First, straightforward analyses are possible, whereas the effects of sheath and secondary electron emission are considered in the analysis of electrostatic probe data. Second, measuring polarization is possible; this is useful for identifying the measured wave.

## 2. Experimental Setup

Wave measurements were performed during plasma

current ramp-up experiments on the TST-2 spherical tokamak ( $R_0 \leq 0.38$  m,  $a \leq 0.25$  m). These experiments were performed in deuterium plasmas with  $B_{t0} \leq 0.1$  T and  $I_p \approx 1.3$  kA. The initial plasma current was generated by ECH (2.45 GHz/5 kW), and subsequently the plasma current was ramped up by the LHW (200 MHz/10 kW) excited by a dielectric-loaded waveguide array antenna (grill antenna) [1, 4].

Each channel of the 5ch-RFMP contain a one-turn loop enclosed in a stainless steel cylinder (diameter of 25 mm) to reject the RF fields coming from unwanted parts of the system. A 2 mm wide and 16 mm long slit present on the front face of the cylinder allows the loop to detect the RF magnetic field. A short ceramic cover over the cylinder physically protects the RFMP from the plasma and reduces its sensitivity to electrostatic fields. Five identical RFMPs, separated by 30 mm from each other, are arranged in a cross configuration, and the assembly is installed on the outboard midplane of TST-2.

A schematic drawing of the 5ch-RFMP polarization and wavevector measurement setup is presented in Fig. 1.

author's e-mail: shinya@fusion.k.u-tokyo.ac.jp

<sup>\*)</sup> This article is based on the presentation at the 23rd International Toki Conference (ITC23).

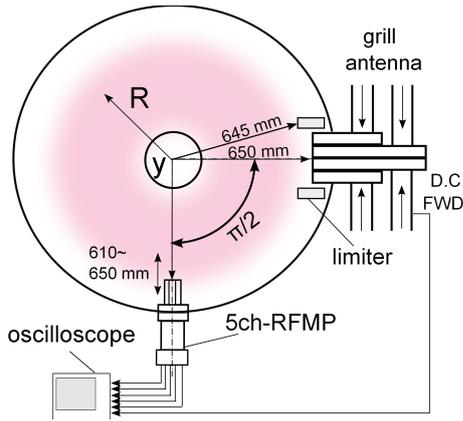


Fig. 1 Schematic arrangement of the 5ch-RFMP polarization and wavevector measurement system viewed from the top. Counter-clockwise direction is defined as the positive direction of the wave travel.

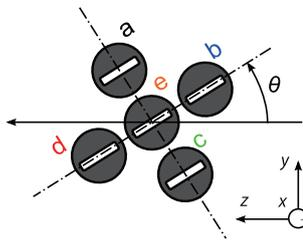


Fig. 2 The 5ch-RFMP as viewed from the plasma, with the definition of the axes and the slit orientation angle  $\theta$  and the name of each RFMP.

The  $y$ -axis is parallel to the symmetry axis of the torus (i.e., the vertical axis), the  $z$ -axis is in the toroidal direction (positive direction is defined counterclockwise as viewed from the top), and the  $x$ -axis is in the negative major radial direction (Fig. 2) with the origin at  $R = 0.645$  m. The five channels are referred to as  $a$ -RFMP- $e$ -RFMP. The angle  $\theta$  defines the direction of the slits relative to the toroidal direction (i.e., the  $z$ -axis) (Fig. 2). When  $\theta = 0$ , the toroidal component is measured by the RFMP. The vertical position of the 5ch-RFMP is at  $y = 0$  m (i.e., on the midplane), and the radial position can be varied on a shot-by-shot basis in the range  $R = 0.61 - 0.65$  m. The toroidal location of the 5ch-RFMP is  $90^\circ$  clockwise from the grill antenna. The output signals of the five channels are digitized using an oscilloscope (1 G Samples/s, 8 MWords). The cable lengths for the five channels are adjusted to be the same to ensure accurate phase measurements.

The forward (FWD) signal of the directional coupler (D.C.) measured in one of the transmission lines to the grill antenna was used as the reference of phase measurement, which is essential to measure  $k_x$  from a shot-by-shot radial position scan of the 5ch-RFMP. The front surface of the movable private limiter surrounding the grill antenna was located at  $R = 0.645$  m (measured on the midplane), and the front face of the grill antenna was at  $R = 0.650$  m. Pos-

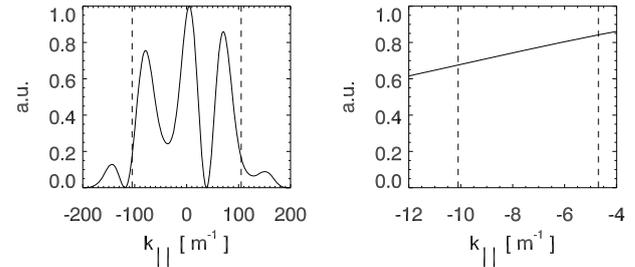


Fig. 3 The parallel wavenumber ( $k_{\parallel}$ ) spectrum in front of the grill antenna. The 5ch-RFMP can detect  $|k_{\parallel}| < 105$   $\text{m}^{-1}$ . The figure on the right shows the  $k_{\parallel}$  spectrum on an expanded scale.

itive  $k_{\parallel}$  is defined in the direction of the wave travel in the counter-clockwise direction. The line integrated density ( $N_e l$ ) is measured using a microwave interferometer with a radial line of sight at  $y = 0$ . The density at  $y = 0$ ,  $R = 0.64$  m was measured by an electrostatic probe.

The angular ( $\theta$ ) scan was performed (every  $\pi/8$  rad) at  $R = 0.61$ ,  $0.63$ , and  $0.65$  m. The launched wavenumber spectrum can be varied by adjusting the phase of the RF wave at each waveguide of the grill antenna. In this experiment, the phases were adjusted to have a broad wavenumber spectrum (Fig. 3). The spectrum was not appropriate for the current drive and the driven plasma current was low (1.3 kA). The density measured by the electrostatic probe at  $R = 0.64$  m was  $1 \sim 10 \times 10^{15} \text{ m}^{-3}$ . The toroidal magnetic field strength was 0.04 T at  $R = 0.63$  m. The line integrated density at  $y = 0$  m was  $1.5 \times 10^{16} \text{ m}^{-2}$ . These values were used to solve the dispersion relation.

### 3. Wave Measurement Data

Results of the wave measurements by the 5ch-RFMP at  $R = 0.61$ ,  $0.63$ , and  $0.65$  m are presented in Fig. 4. Data obtained by  $a$ -RFMP are not provided because the wave measurement (especially phase) by this probe was inaccurate owing to a loose connection. The first row exhibits the squared voltage at 200 MHz measured by the 5ch-RFMP (averaged over four RFMPs). The horizontal axis is the normalized angle  $\theta/2\pi$ . The angular dependence of the squared voltage is nearly  $\cos^2(\theta - \pi/2)$  at all radial positions, indicating that the poloidal RF magnetic field is dominant.

The data presented in the top row are fitted by a function of the form  $A_0^2 \cos^2(\theta - A_1) + A_2$ , where  $A_0$  is the amplitude of the measured wave,  $A_1$  represents the angle between the background and the wave magnetic field in the  $y$ - $z$  plane, and  $A_2$  is the offset. Table 1 exhibits the measured angle of polarization. Because the  $x$  component should not depend on  $\theta$ , the offset is likely generated by the sensitivity to the  $x$  component. Thus, to obtain the amplitude and the polarization accurately, a rotational scan is crucial. The second row in Fig. 4 presents  $\Delta\phi_{c-e}$  (green), the phase difference between  $c$ -RFMP and  $e$ -RFMP. The

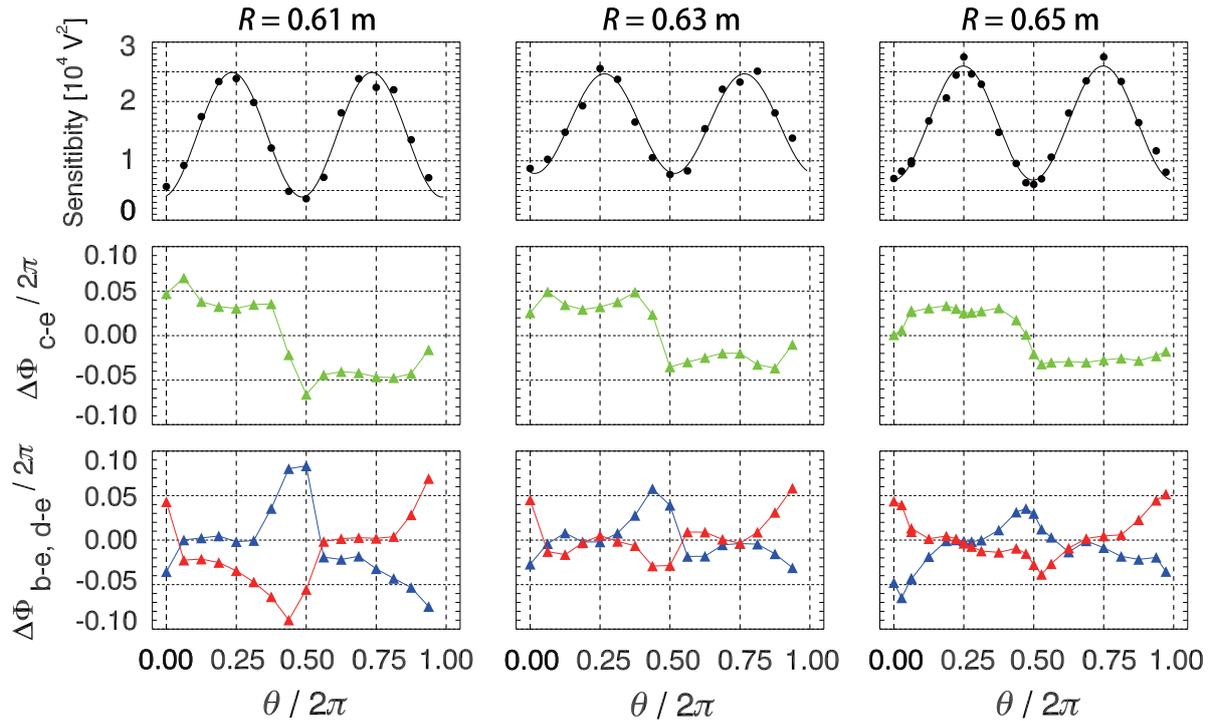


Fig. 4 Squared voltage (top) and phase differences between e and other channels (2nd and 3rd rows) at 200 MHz plotted as functions of the normalized angle  $\theta/2\pi$ . The green, blue, and red symbols represent  $\Delta\phi_{c-e}$ ,  $\Delta\phi_{b-e}$ , and  $\Delta\phi_{d-e}$ , respectively.

Table 1 Measured angle of polarization at three major radii.

$R$ [m]	$A_1/2\pi$
0.61	$0.235 \pm 0.001$
0.63	$0.266 \pm 0.002$
0.65	$0.248 \pm 0.002$

third row presents the phase differences  $\Delta\phi_{b-e}$  (blue) and  $\Delta\phi_{d-e}$  (red). These phase differences and spacings between different channels or locations are used to calculate the components of the wavevector.

#### 4. Discussion

Here, we analyze only the dominant component of  $B$  (i.e.,  $y$  component of  $B$ ). Data in the ranges  $\pi/2 - \pi/8 \leq \theta_p \leq \pi/2 + \pi/8$  and  $3\pi/2 - \pi/8 \leq \theta_p \leq 3\pi/2 + \pi/8$  are used. Assuming that the same wave component is detected by the RFMPs, the analyzed values from these ranges are averaged and the uncertainty is derived from the scatter of these values.

The  $x$ ,  $y$  and  $z$  components of the wavevector are calculated using the following equations,

$$k_y = \langle (\Delta\phi_{b-e} - \Delta\phi_{d-e}) / 2L \sin \theta \rangle_{|\theta=\theta_p}, \quad (1)$$

$$k_z = \langle -\Delta\phi_{c-e} / L \sin \theta \rangle_{|\theta=\theta_p}, \quad (2)$$

$$k_x = \langle d\Delta\phi_{\text{ref}-e} / dx \rangle_{|\theta=\theta_p}, \quad (3)$$

where  $L = 0.03$  m is the distance between  $e$ -RFMP and other RFMPs. Taking the FWD signal of the D.C. as the

Table 2 Measured wavevector components at  $\theta = \theta_p$ .

$R$ [m]	$k_{\parallel}$ [ $\text{m}^{-1}$ ]	$k_{\perp}$ [ $\text{m}^{-1}$ ]
0.61	$-8.6 \pm 1.5$	...
0.62	...	$12.5 \pm 2.0$
0.63	$-6.3 \pm 1.6$	$12.8 \pm 1.1$
0.64	...	$12.9 \pm 1.2$
0.65	$-6.2 \pm 0.7$	...

phase reference,  $|dx|$  is 0.02 m and the measured locations were  $R = 0.61, 0.63, \text{ and } 0.65$  m. Note that we can assume  $k_{\parallel} \approx k_z$  (component parallel to the magnetic field) in this experiment because the pitch angle of the magnetic field is almost zero. In addition, the calculated value of  $k_y$  is almost zero. Hence, we can consider  $k_{\perp} \approx |k_x|$  (component perpendicular to the magnetic field). Table 2 illustrates the derived wavevector components and standard deviations.

The range of the derived  $k_{\parallel}$  (represented by the dashed lines in Fig. 3 right) corresponds to the central spectral component among the launched components (Fig. 3 left). Although the 5ch-RFMP can detect  $|k_{\parallel}| < 105 \text{ m}^{-1}$ , the waves with  $k_{\parallel} \sim -80, 70 \text{ m}^{-1}$  were not observed. This fact implies that waves with such high  $k_{\parallel}$  were absorbed by the plasma prior to detection by the probe, which is separated  $90^\circ$  toroidally from the antenna.

The measured  $|k_{\perp}|$  at  $R = 0.63$  m can be compared with that calculated from the cold plasma dispersion relation [5] using  $B_t = 0.04$  T and  $k_{\parallel} = 6.3 \pm 1.6 \text{ m}^{-1}$ . Because the electron density ( $n_e$ ) is not known very accurately,  $|k_{\perp}|$  was

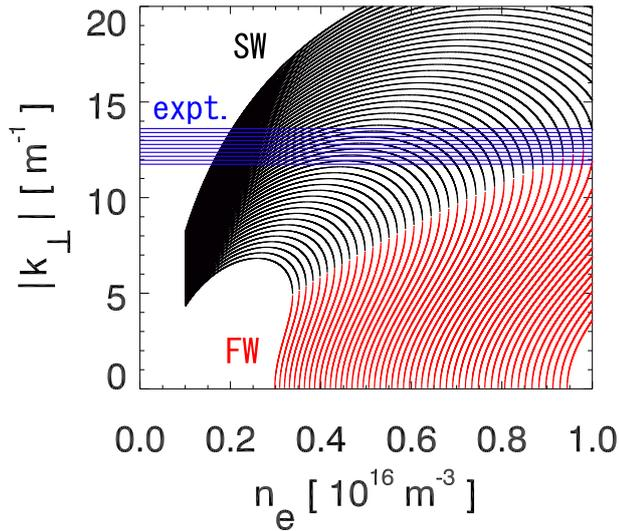


Fig. 5 The cold plasma dispersion relation. Black lines represent the SW. Red lines represent the FW.  $|k_{\perp}|$  is calculated from the dispersion relation using the measured  $k_{\parallel}$  at  $R = 0.63$  m,  $B_t = 0.04$  T, and  $n_e$  in the range  $10^{15-16} \text{ m}^{-3}$ . The blue lines mark the range of measured  $|k_{\perp}|$  at  $R = 0.63$  m.

calculated for  $n_e$  within the range  $10^{15-16} \text{ m}^{-3}$ . Figure 5 illustrates the dispersion relation. The black and red curves represent the slow wave (SW) and fast wave (FW), respectively. We can observe that SW has larger values of  $|k_{\perp}|$  than FW, and FW has a cutoff (where  $|k_{\perp}| = 0$ ) at higher densities. The blue lines represent the range of measured  $|k_{\perp}|$  at  $R = 0.63$  m. The measured  $|k_{\perp}|$  is consistent with that of the SW.

## 5. Conclusions

Wave identification was performed using the data obtained by 5ch-RFMP during LHW injection experiments on TST-2. The polarization angle was successfully measured, and the result indicates that the poloidal RF magnetic field is dominant.  $k_{\parallel}$  calculated from the phase differences between different channels of the 5ch-RFMP was consistent with the launched  $k_{\parallel}$  spectrum. Although the 5ch-RFMP can detect  $|k_{\parallel}| < 105 \text{ m}^{-1}$ , wave components with  $k_{\parallel} \sim -80, 70 \text{ m}^{-1}$  were not observed, implying that the waves with such high  $k_{\parallel}$  were absorbed by the plasma before they reached the probe located  $90^\circ$  toroidally away from the antenna. The comparison of the measured  $|k_{\perp}|$  at  $R = 0.63$  m and the  $|k_{\perp}|$  calculated from the dispersion relation using the measured  $|k_{\parallel}|$  at  $R = 0.63$  m indicated that the measured wave is the SW.

## Acknowledgment

This work was supported by Japan Society for the Promotion of Science (Grants-in-Aid for Scientific Research (S) (21226021)) and by the National Institute for Fusion Science (NIFS) Collaborative Research Program No. NIFS10KOAR012.

- [1] Y. Takase, A. Ejiri *et al.*, Nucl. Fusion **53**, 063006 (2013).
- [2] T. Takahashi, S. Takamura and T. Okuda, J. Appl. Phys. **53**, 6693 (1982).
- [3] K. Ushigusa, S. Takamura and T. Okuda, Nucl. Fusion **24**, 751 (1984).
- [4] T. Wakatsuki, A. Ejiri *et al.*, AIP Conference Proceedings **1406**, 431 (2011).
- [5] T.H. Stix, *Waves in Plasmas* (Chapter I) (American Institute of Physics, 1992).